Integration and control of lithium-ion BESSs for active network management in smart grids: Sundom smart grid backup feeding case

Author(s):   Parthasarathy, Chethan; Hafezi, Hossein; Laaksonen, Hannu

Title: Integration and control of lithium-ion BESSs for active network management in smart grids: Sundom smart grid backup feeding case

Year: 2021

Version: Publisher's PDF

Please cite the original version:

Parthasarathy, C., Hafezi, H. & Laaksonen, H. (2021). Integration and control of lithium-ion BESSs for active network

management in smart grids: Sundom smart grid backup feeding case. *Electrical Engineering*, 1-15. https://doi.org/10.1007/s00202-021-01311-8

ORIGINAL PAPER

Integration and control of lithium-ion BESSs for active network management in smart grids: Sundom smart grid backup feeding case

Chethan Parthasarathy[1] · Hossein Hafezi[2] · Hannu Laaksonen[1]

Abstract

Lithium-ion battery energy storage systems (Li-ion BESS), due to their capability in providing both active and reactive power services, act as a bridging technology for efficient implementation of active network management (ANM) schemes for land-based grid applications. Due to higher integration of intermittent renewable energy sources in the distribution system, transient instability may induce power quality issues, mainly in terms of voltage fluctuations. In such situations, ANM schemes in the power network are a possible solution to maintain operation limits defined by grid codes. However, to implement ANM schemes effectively, integration and control of highly flexible Li-ion BESS play an important role, considering their performance characteristics and economics. Hence, in this paper, an energy management system (EMS) has been developed for implementing the ANM scheme, particularly focusing on the integration design of Li-ion BESS and the controllers managing them. Developed ANM scheme has been utilized to mitigate MV network issues (i.e. voltage stability and adherence to reactive power window). The efficiency of Li-ion BESS integration methodology, performance of the EMS controllers to implement ANM scheme and the effect of such ANM schemes on integration of Li-ion BESS, i.e. control of its grid-side converter (considering operation states and characteristics of the Li-ion BESS) and their coordination with the grid side controllers have been validated by means of simulation studies in the Sundom smart grid network, Vaasa, Finland.

Keywords Active network management · Battery energy storage systems · Lithium-ion battery · Energy management systems · Equivalent circuit model · Power electronics converter controls

1 Introduction

Stochastic and unpredictable nature of the renewable energy sources (RES) and their geographic distribution, often in remote areas with weak electricity distribution network, induce various grid-related challenges. In such situations, managing power balance and grid stability is nonetheless a challenging task, as these factors depend on a number of variables depending on the network topology [1–3]. Challenge of supply reliability and quality with higher integration of RESs has been tried to address by setting stricter grid code requirements and innovative grid control architectures such as active network management (ANM) schemes [4, 5].

Therefore, ANM schemes are utilized to improve the penetration of RESs by managing available flexibilities in the distribution grids and keeping their power quality within the acceptable limits defined by the grid codes [6, 7].

In order to implement ANM schemes, distributed energy resources (DERs) in the distribution network (i.e. MV and LV systems) play an important role in providing flexibility in the power system for local and system wide grid resiliency, along with maximizing network DER hosting capacity [8, 9]. These flexibilities consist of active power (*P*-) control and reactive power (*Q*-) control of flexible resources like controllable DER units, battery energy storage systems (BESS), controllable loads and electric vehicles (EVs) which are connected in distribution networks, thereby providing different local and system-wide technical services as part of future ANM schemes [4, 10, 11].

BESSs play a major role as flexible energy source (FES) in ANM schemes by bridging gaps between non-concurrent renewable energy sources (RES)-based power generation and demand in the MV and low-voltage (LV) distribution

✉ Chethan Parthasarathy
  chethan.parthasarathy@uwasa.fi

1 School of Technology and Innovations, Flexible Energy Resources, University of Vaasa, Vaasa, Finland

2 Faculty of Information Technology and Communication Sciences, Tampere University, Tampere, Finland

networks. Ability of the BESS to provide both active power and reactive power flexibility services makes them a multipurpose FES for ANM needs [12–14]. With current technological maturity, Li-ion BESSs are capable of acting as a cost-efficient FESs and provide multiple technical ancillary/flexibility services like frequency control by controlling active power injection and voltage control by active/reactive power management [15, 16]. From transmission and distribution system operators (TSO/DSOs) point of view, an effective way to utilize BESS for ANM will be to place them in a HV/MV substation or in the MV distribution, e.g. at MV/LV substations. Hence, Li-ion BESSs will be an integral part of the ANM scheme at the MV distribution system for this study.

Efficient operation of ANM schemes highly bank upon the design of energy management system (EMS) [17, 18] which manages the available flexibilities in the distribution system. However, intermittent nature of the RES-based flexible DERs narrows the flexibility provisioning for ANM schemes, thereby challenging their scope of services. Hence, a highly controllable FES will be needed to design the EMS functionalities effectively. Therefore, Li-ion BESSs due to their fast and controllable dynamics will play an important role in the EMS functionalities for multiple flexibility services acting as a buffer to manage flexibilities in the distribution systems.

In [19–23], extensive research on various ANM schemes to maintain system voltage level, as well as to manage the reactive power flow from the DERs within the reactive power window (RPW) provided by the Finnish TSO, Fingrid and ENTSO-E network code [24], have been studied and validated in a local smart grid pilot SSG. From previous results, the reactive power control of wind turbine generator (WTG) was sufficient in order to satisfy RPW requirements on an hourly average data obtained from the SSG MV distribution network. However, it had been recommended to study multi-use capabilities of BESSs in multi-objective ANM schemes by controlling flexibilities in RESs, BESSs and on-load tap changing transformers (OLTCs) [25–27] on a smaller time-step in order to design ANM schemes and services effectively. It was also suggested to study the effect of load curves BESS integration methodology (i.e. the effect of ANM load on the Li-ion BESS converter controllers).

Therefore, the objective of this study is to validate the overall role of Li-ion BESS integration design and its stability for ANM needs, which is often used to mitigate transient instability. Hence, a rule-based [28] EMS has been proposed in Sect. 4 to study the overall power system stability by means of electromagnetic transient (EMT) simulation studies in Matlab/Simulink (SimPowerSystems). Developed EMS design for ANM in the MV distribution system will be based on managing two key network parameters. First objective of the EMS will be to manage reactive power flow from the DERs between the TSO/DSO interface defined by the reactive power window (RPW) provided by Finnish TSO, Fingrid, and ENTSO-E network codes [24]. The reactive power flow between TSO/DSO interfaces has to comply with the RPW limits to avoid being penalized. Second objective is to manage the MV network voltages which are facing higher fluctuation due to RESs in the network, between the limits set by grid codes. Hence, maintenance of voltage and RPW limits defined by the grid code provides a strong case for implementation of ANM schemes to administer technical ancillary services by effectively managing active and reactive power flows from the available FESs in the distribution network.

To conduct such studies, the requirements are (a) development of accurate Li-ion BESS performance model, (b) Li-ion BESS integration methodology (i.e. design and development of controllers for the power electronic interfaces used for the grid integration purposes) and (c) EMS design (i.e. development of co-ordinated control of grid side controllers with DER controllers).

Design and methodology for integration of Li-ion BESS in the MV distribution system, which are capable to capture and study the fast transient dynamics by means of EMT simulations (i.e. smaller time step system simulation), have been developed and presented in [29, 30]. Hence, in this paper, the developed Li-ion BESS integration design is subjected to the active and reactive power requirements provided by the EMS implementing ANM scheme. EMS focus has been laid on designing coordinated control between the grid side controllers (i.e. the EMS controllers) and Li-ion BESS converter controllers. To validate the developed ANM scheme and the Li-ion BESS integration design, the backup feeding use case in the SSG has been modelled. Under this use case condition, the voltages and the RPW window limits are expected to be under duress, especially at low WTG, which will be addressed by the available flexibility (i.e. Li-ion BESS and WTG) in the MV distribution system with the help of developed EMS thereby providing active network management services.

To summarize, in this paper, the focus has been laid on,

1. Development of EMS architecture for ANM with *QU-*, BESS *PU-*, WT *PU-* and on-load-tap-changer (OLTC) controllers for managing available flexibilities of various DERs, especially to generate control signals for the Li-ion BESS and WTG converters connecting them to the MV distribution system,
2. Utilization of accurate equivalent circuit model (ECM) for Li-ion BESS controller development in grid integration studies
3. Evaluation of Li-ion BESS integration design (i.e. effects of BESS DC/AC voltage source converter and

DC/DC bidirectional buck-boost converter controllers for the ANM load requirements)

4. Understanding simultaneous converter interactions between (a) converter + Li-ion BESS, and (b) converter + network management (ANM scheme).

This paper has been organized in the following manner. Sundom smart grid network architecture has been explained in Sect. 2. The reason for underlying voltage fluctuations in the network is presented in Sect. 3. Section 4 explains the ANM architecture and the developed EMS design to manage FESs in the MV distribution system. Developed ANM scheme and their performance with respect to the co-ordinated control attributes have been validated by means of case studies in Sect. 5.

2 Sundom smart grid network

SSG is represented in Fig. 1, which is a pilot living laboratory jointly created by ABB, Vaasan Sähköverkko (DSO), Elisa (communications) and University of Vaasa. Real-time voltage and current measurements (IEC 61,850 standard) are recorded from the MV distribution network, from all four feeders at a HV/MV substation and from three MV/LV substations comprising 20 measurement points in total. Measurement is sampled at 80 samples/cycle. In addition, active and reactive power, frequency, RMS voltages and current

Fig. 1 SSG network diagram

measurements are received by GOOSE messages. SSG is modelled accurately with available data and grid structure, i.e. distribution network structure, loads, generation units, etc., obtained from the local DSO Vaasan Sähköverkko.

Wind power generation is modelled from the measured active power (P_{WIND}) and reactive power (Q_{WIND}) at bus Tuulivoima (J08), on 30-May-2017. P_{WIND} and Q_{WIND} are then converted to system currents, with MV voltage as reference as explained in [31]. Loads at Sulva (J06), Sundom (J07) and Vaskiluoto (J09) feeders are modelled as per the measured data from the MV distribution system.

Li-ion BESS dynamic characteristics were modelled accurately by considering the influence of parameters such as temperature, depth of discharge and C-rate (charge/discharge) by means of second-order equivalent circuit cell model [30]. Li-ion BESS is connected to the power system by means of power electronic interface. In this case, DC/DC bidirectional buck-boost converter will stabilize fluctuating/changing battery voltage. It will also aid in charging and discharging of batteries within its safe operating window. DC/AC -converter will be connected to the high voltage side of the DC/DC -converter, which converts it into 3-phase, 400 V_{RMS}. Voltage will be boosted to MV level by means of 3-phase transformer thereby completing integration of the battery system.

Deriving accurate design of the power converter controllers, i.e. DC/AC voltage-source-converter (VSC) and DC/DC BESS buck-boost controllers for optimal operations is imperative considering the nature of applications they are tending in this study. Overall BESS integration design and their integration methodology along with power electronics controller design are explained in [30]. Developed ANM scheme in Sect. 4 will be utilized to manage flexibilities from WT generator, Li-ion BESS and the HV/MV OLTC transformer in SSG and will be validated in the use case where the loads are varying at low WT generation.

3 Problem description—voltage fluctuation

The intermittency of renewable power generation (i.e. wind power in SSG) introduces negative effects on the distribution grid, especially in terms of voltage rise and drop issues [32]. To understand the voltage change issues in the MV network of the SSG, an equivalent circuit of the network is deduced in Fig. 2. The line impedance (Z_{Grid}) is represented as R_{Grid} and X_{Grid}. The current flow at the point of current coupling (PCC), i, is represented as, I_i, and the MV bus voltage is measured as U_{MV}. Wind turbine generator and Li-ion BESS have been represented as current sources with output, I_{Wind} and I_{BESS}. The loads in SSG are represented as current sinks, consuming I_{Su}, I_{Sun} and I_{Vas}.
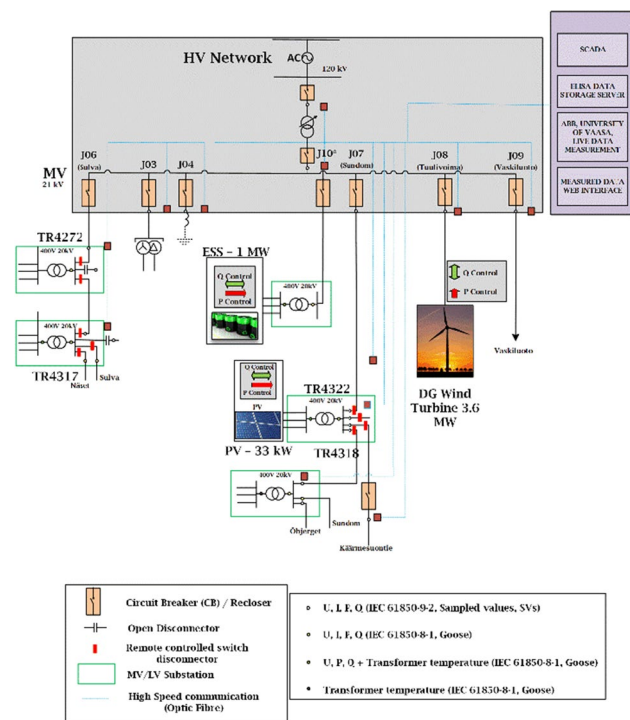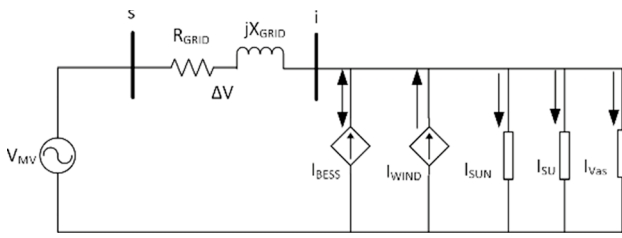
Fig. 2 Equivalent circuit representation of SSG

Eqs. (1)–(6) represent the power flow in the SSG network. The active power flow at the PCC has been represented by (1) and summarized as in (2), where P_{Wind}, P_{BESS} and P_{Load} represent the active power contribution from the WTG, Li-ion BESSs and load power consumption, respectively. P_{Load} includes the active power flows of the individual load feeders from Sulva, Sundom and Vaskiluoto (P_{Su}, P_{Sun} and P_{Vas}). Similarly, reactive power flow at the PCC is shown in (3), where Q_{Wind}, Q_{BESS} and Q_{Load} represent the reactive power contribution from the WTG, Li-ion BESSs and load power consumption, respectively. Q_{Load} includes the reactive power flows of the individual load feeders from Sulva, Sundom and Vaskiluoto (Q_{Su}, Q_{Sun} and Q_{Vas}). Equation (4) represents the current distribution at the PCC in the network. Overall power flow at the PCC is shown in (5), where S_i determines the apparent power flow, P_i and Q_i shows their active and reactive power flow components. The injected current at the PCC is represented in (6).

The equivalent circuit for Fig. 1 can be represented as (7), where U_{MV} represents the MV grid voltage and the ΔV determines the voltage deviation in the MV grid. Voltage at the PCC is represented by U_i in (8) and substituting Z_{Grid} values (9) is obtained representing voltage at the PCC.

$$P_i = P_{Wind} \pm P_{BESS} - P_{Sun} - P_{Su} - P_{Vas} \tag{1}$$

$$P_i = P_{Wind} \pm P_{BESS} - P_{Load} \\ \text{where, } P_{Load} = P_{Sun} + P_{Su} + P_{Vas} \tag{2}$$

Similarly,

$$Q_i = \pm Q_{Wind} \pm Q_{BESS} - Q_{Load} \\ \text{where, } Q_{Load} = Q_{Sun} + Q_{Su} + Q_{Vas} \tag{3}$$

$$I_i = \pm I_{Wind} \pm I_{BESS} - I_{Load} \tag{4}$$

$$S_i = P_i + jQ_i = U_i \cdot I_i \tag{5}$$

$$I_i = \left(\frac{S_i}{U_i}\right) = \frac{P_i - jQ_i}{U_i} \tag{6}$$

Substituting current I_i from Eqs. (6) to (9), the overall voltage deviation is represented in (10). The voltage deviation ΔU is influenced by both active and reactive power flows in the network. By resolving (10), Eq. (11) is obtained, which shows the voltage deviation due to active power component (ΔU_d) and reactive power component (ΔU_q).

$$U_{MV} = U - I_i Z_{Grid} \tag{7}$$

$$U_i = U_{MV} + I_i Z_{Grid} \tag{8}$$

$$U_i = U_{MV} + I_i(R_{Grid} + jX_{Grid}) = U_{MV} + \Delta U \tag{9}$$

$$\Delta U = \frac{P_i \cdot R_{Grid} + Q_i \cdot X_{Grid}}{|U_i|} + j\frac{P_i \cdot X_{Grid} - Q_i \cdot R_{Grid}}{|U_i|} \tag{10}$$

i.e.
$$\Delta U_d = \frac{P_i \cdot R_{Grid} + Q_i \cdot X_{Grid}}{|U_i|} \\ \Delta U_q = \frac{P_i \cdot X_{Grid} - Q_i \cdot R_{Grid}}{|U_i|} \tag{11}$$

In the SSG's MV power grid, the magnitude of ΔU_q is comparatively smaller than ΔU_d but their contribution to voltage deviation is higher than that of the LV distribution system due to the line reactance. However, the purpose of this study is to design and develop effective utilization of Li-ion BESS active power control and to understand and map the effects of MV grid voltage fluctuation on Li-ion BESS and its adjoining power electronic converter controls. Hence, the effect of ΔU_q is assumed a constant value. Therefore, by substituting active components of active power flow at the PCC, (12) has been obtained. The magnitude of voltage deviation $|\Delta U_i|$, at PCC is represented in (13). It is noted that the only controllable flexible energy source in Eqs. (12) and (13) is the Li-ion BESS, and hence it plays an immense role in regulating voltages in MV distribution network. By substituting Eqs. (12) in (13), we obtain the equation to provision the required change in voltage in (14).

$$\Delta U_d = \frac{(P_{Wind} \pm P_{BESS} - P_{Load}) \cdot R_{Grid} + Q_i \cdot X_{Grid}}{|U_i|} \tag{12}$$

$$|\Delta U_i| = |U_{MV}| + |\Delta U_d| \tag{13}$$

$$|\Delta U| = |U_{MV}| + \frac{(P_{Wind} \pm P_{BESS} - P_{Load}) \cdot R_{Grid} + Q_i.X_{Grid}}{|U_i|} \tag{14}$$

Finally, by rearranging the equation, we obtain magnitude of active power discharge required from BESSs, i.e. in (15) to regulate the required voltages in the MV distribution system. Positive value of P_{BESS} describes battery charging and

the negative value to that of battery charging. Equation (15) shall form the basis for Li-ion BESS dispatch control operation in the study. The value of ΔU_i is as shown in (16), which is the difference between voltage at bus i and U_{ref} defines the required voltage correction factor at the MV bus.

$$P_{BESS} = (|\Delta U_i| - |U_{MV}|) \cdot \left[\frac{|U_{MV}|}{R_{Grid}}\right] - Q_i \cdot \left[\frac{X_{Grid}}{R_{Grid}}\right] + P_{Load} - P_{Wind} \tag{15}$$

$$|\Delta U_i| = |U_i| - |U_{ref}|, \tag{16}$$

where U_{ref} is the voltage limits set by grid codes.

4 ANM Architecture and EMS Design

In this paper, the ANM management scheme is developed in reference to managing flexibilities from Li-ion BESSs and WT generators in the MV distribution system of SSG. Section 4.1 provides an explanation on the reactive power window requirements in TSO/DSO interface, which forms an inherent condition to be maintained as a part of ANM scheme, along with system voltages and frequency. Developed ANM scheme for Li-ion BESS operation and other available flexibilities in the MV distribution grid is explained in Sect. 4.2 and 4.3 shows the EMS architecture.

4.1 Reactive power window

Based on SSGs existing data, the future reactive power window at the MV side of the HV/MV transformer and its limits are presented in Fig. 3 [20]. The reactive power window and microgrid requirements are combined for the MV distribution system. Limits for the maximum active power are based on the measured data of the year 2016, when $P_{MAX,IMPORT}$ was 8.3 MW and $P_{MAX,EXPORT}$ was 1.975 MW. Apart from
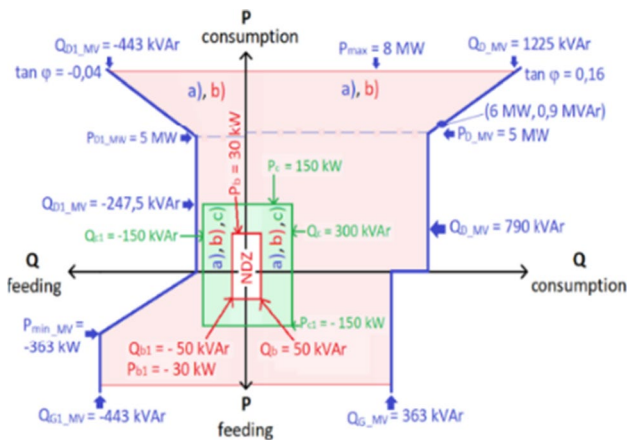
the Fingrid's requirements, EU legislations dictate reactive power interactions between TSOs and DSOs. TSO may require DSOs to actively control the exchange of reactive power and subsequently, DSO may require the TSO to consider utilizing the distribution network for reactive power management. The actual reactive power range should not exceed 48% of maximum capacity to import or export of active power (P_{max}), when importing (consuming) reactive power $\cos\varphi_{max}$ at $0.9_{inductive(ind)}$ and exporting (producing) reactive power $\cos\varphi_{max}$ at $0.9_{capacitive(cap)}$. In addition, TSO cannot export reactive power when active power import is below $0.25*P_{max}$ as [22]. ANM voltage control threshold is shown in Fig. 4, where the maximum voltage is set at 1.05 pu and the minimum voltage limits are set at 0.95 pu (both HV and MV connection points), which is based on the thermal limit for maximum current flow in the system.

4.2 ANM Architecture design—SSG

Flexibilities provided by the wind turbine (WT) are dependent on its active power generation, which in turn is dependent on the intermittent nature of wind. Thereby, WT alone will not be reliable enough to provide flexibility services in the MV distribution system of SSG. Hence, the Li-ion BESS which is placed strategically in the MV distribution grid will be able to complement WTG in providing various flexibility services in a smart grid.

BESSs when integrated into the MV distribution system of the SSG are primarily designed to complement stochastic nature of wind power generation, i.e. store excess wind power generation and discharge during reduced wind power generation and secondarily used in providing technical ancillary services. Li-ion BESSs have multi-use capability based on their characteristics and hence the ANM scheme developed in this paper is inclusive utilizing such capabilities. The technical ancillary services in the ANM scheme are designed based on the available flexibilities in the MV distribution system. In this case, ancillary services include,
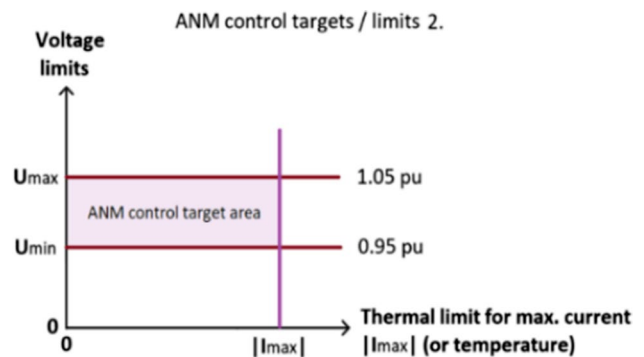

Fig. 3 Reactive power window for SSG at MV (FINGRID)

Fig. 4 Voltage control targets at HV and MV connection points

1. Voltage regulation within the threshold (Fig. 4) in the MV distribution system, mainly in all the MV feeders, is the primary objective of this ANM architecture
2. Maintaining the RPW defined by the Finnish TSO, Fingrid, at the HV side of the SSG is defined in Sect. 4.1. Reactive power flow will be controlled from the available FESs to avoid violation of grid codes, thereby supporting customers to avoid paying the penalty fees to the TSO.

4.3 Energy management system

The most important layer of operation in the ANM scheme is the energy management system (EMS)

which concerns with the operation of active and reactive power flows between MV grid and flexible energy sources, in this case, Li-ion BESS and WT generator. Objective of the EMS is to maintain $\underline{U}_{grid,ref}$ within the limits specified by grid codes by controlling the active and reactive power flows at the DSO/TSO interface, especially focusing on the reactive power flow which has been maintained within the limits defined by RPW.

The ANM control architecture described in Fig. 5 is designed for implementation in SSG. Measured MV grid data such as active power ($P_{grid,meas}$), reactive power ($Q_{grid,meas}$), voltages ($U_{grid,meas}$), frequency ($f_{grid,meas}$) are given as input to the EMS layer. Primary role of the EMS
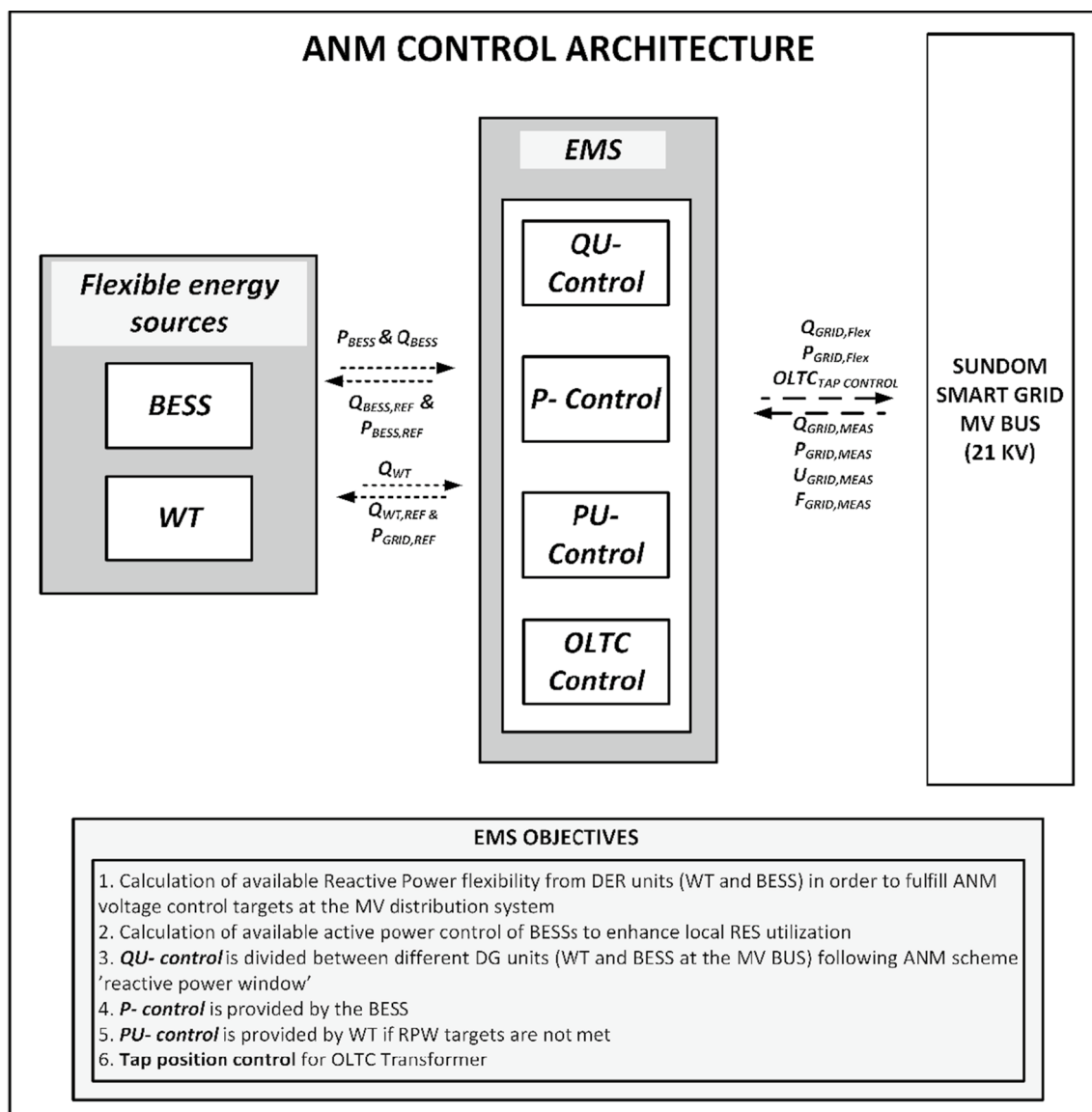

Fig. 5 ANM architecture

is to constantly monitor the reference parameters in the MV distribution system. If any of the parameters, i.e. $Q_{grid,ref}$ and $U_{grid,ref}$ are not within the defined threshold values, EMS's secondary functionality of managing the available flexibilities in the MV power system is utilized by generating reference control signals for the various grid side controllers. The grid side controllers that participate in ANM are *QU-*, BESS-*PU-*, WT

$$Q_{wind,min} \leq Q_{wind} \leq Q_{wind,max}$$

$$\text{where,} \begin{cases} Q_{wind,min} = -\sqrt{S_{wind}^2 - P_{Wind}^2} \\ Q_{wind,max} = \sqrt{S_{wind}^2 - P_{Wind}^2} \end{cases} \quad (17)$$

$$Q_{BESS,min} \leq Q_{BESS} \leq Q_{BESS,max}$$

$$\text{where,} \begin{cases} Q_{BESS,min} = -\sqrt{S_{BESS}^2 - P_{BESS}^2} \\ Q_{BESS,max} = \sqrt{S_{BESS}^2 - P_{BESS}^2} \end{cases} \quad (18)$$

$$Q_{flex} = \begin{cases} Q_{MV} - Q_{rpw,max}; (\text{if } V_{SUL} \langle 0.95PU \text{ and } Q_{MV} \rangle Q_{rpw,max}) \\ Q_{rpw,max} - Q_{MV}; (\text{if } V_{SUL} > 1.05PU \text{ and } Q_{MV} < Q_{rpw,min}) \\ 0 \end{cases}$$
$$(19)$$

$$Q_{wind} = \begin{cases} Q_{flex}; (\text{if } Q_{flex} > 0 \text{ and } Q_{flex} < Q_{wind,max}) \\ Q_{wind,max}; (\text{if } Q_{flex} > Q_{wind,max}) \end{cases} \quad (20)$$

$$Q_{BESS} = \begin{cases} Q_{flex} - Q_{wind,max}; (\text{if } Q_{flex} > Q_{wind,max} \\ 0 \end{cases} \quad (21)$$

$$P_{dis} = \begin{cases} P_{REF}; (\text{if } P_{REF} < 1 MW \text{ and } SOC_{min} < SOC < SOC_{max}) \\ 1 MW; (P_{REF} \geq 1 MW \text{ and } SOC_{min} < SOC < SOC_{max}) \\ 0; (\text{if } SOC \leq SOC_{min}) \end{cases}$$
$$(22)$$

$$P_{chg} = \begin{cases} 0; \text{if } SOC > SOC_{max} \\ P_{chg}; \text{if } SOC_{min} < SOC < SOC_{max} \end{cases} \quad (23)$$

PU- control and OLTC- controllers as shown in Fig. 6. If the voltages, frequency and reactive power flows are well within the limits suggested by grid codes, the controllers in the EMS layer stay inactive. However, they constantly monitor the reference parameters in the MV system. In case, the defined MV parameters are out of threshold values ANM scheme starts to activate to mitigate the abnormalities by controlling the grid side controllers. The total required reactive power control is set according to requirements of Fingrid's RPW limits (i.e. Figure 3)

thereby defining the requirements for *QU-* control. The reactive power flexibility in the *QU-* control is provided by Li-ion BESS and WT generator, i.e. Q_{WIND} and Q_{BESS}. If reactive power flow in this situation exceeds RPW limits at the TSO/DSO interface, Q_{WIND} is regulated to adjust the values as the priority. If Q_{WIND} isn't sufficient to regulate RPW limits, the Q_{BESS} will be dispatched.

BESS *PU-* control is utilized to control active power flow from the Li-ion BESS. Despite Li-ion BESSs capability of providing both active and reactive power control, they also provide active power flexibility in terms of both charging- and discharging-related services. In case the BESSs are being charged, their active power discharge control is disabled, whereas the reactive power discharge control component remains active.

Therefore, EMS provides $Q_{BESS,ref}$ & $P_{BESS,ref}$ to the BESS and $Q_{WT,ref}$ and $P_{grid,ref}$ to the WTG. In return, based on the.

internal control algorithms for BESS and WT defined in the following section, BESS returns relevant P_{BESS} & Q_{BESS} back to the EMS, whereas WTG returns Q_{WT} back to the EMS. These control signals are then forwarded to the grid side controllers which in turn injects Q_{flex} (Q_{BESS} and Q_{WT}) to the MV bus. Similarly, BESS *PU-* controller provides active power provisioning from the Li-ion BESS, i.e. P_{BESS} in order to regulate voltages at the MV system. WT *PU-* controller is primarily used to curtail excess active power generation from WT and activated when voltages at MV bus is greater than 1.0 pu. The design and architecture of the individual control techniques, i.e. *QU-*, *P-*, *PU-* and OLTC- control techniques employed in the ANM management principle are explained as below.

4.3.1 *QU-* management system

Reactive power (Q_{WIND}) control of WTG system depends on the reactive power output capability. The inverter operating range should be applied accurately before utilizing reactive power control strategy in WTGs. Therefore, the maximum controllable reactive power from the WTG is calculated by (17). $Q_{WIND,MIN}$ and $Q_{WIND,MAX}$ are the maximum and minimum reactive power output from the WTG. Negative symbol denotes absorbing reactive power and that of positive symbol to generate reactive power.

The reactive power control of BESS is defined by the phasor relationship between the battery inverter operating parameters, for several different levels of BESS active power output (P_{BESS}). When S_{BESS} is larger than P_{BESS}, the inverter can supply or consume reactive power, Q_{BESS}. The BESS inverter can dispatch Q_{BESS} quickly (on the cycle-to-cycle time scale) providing a mechanism for rapid voltage regulation. As the output, P_{BESS}, approaches S_{BESS}, the range of available Q_{BESS} decreases to zero, as shown in (18).
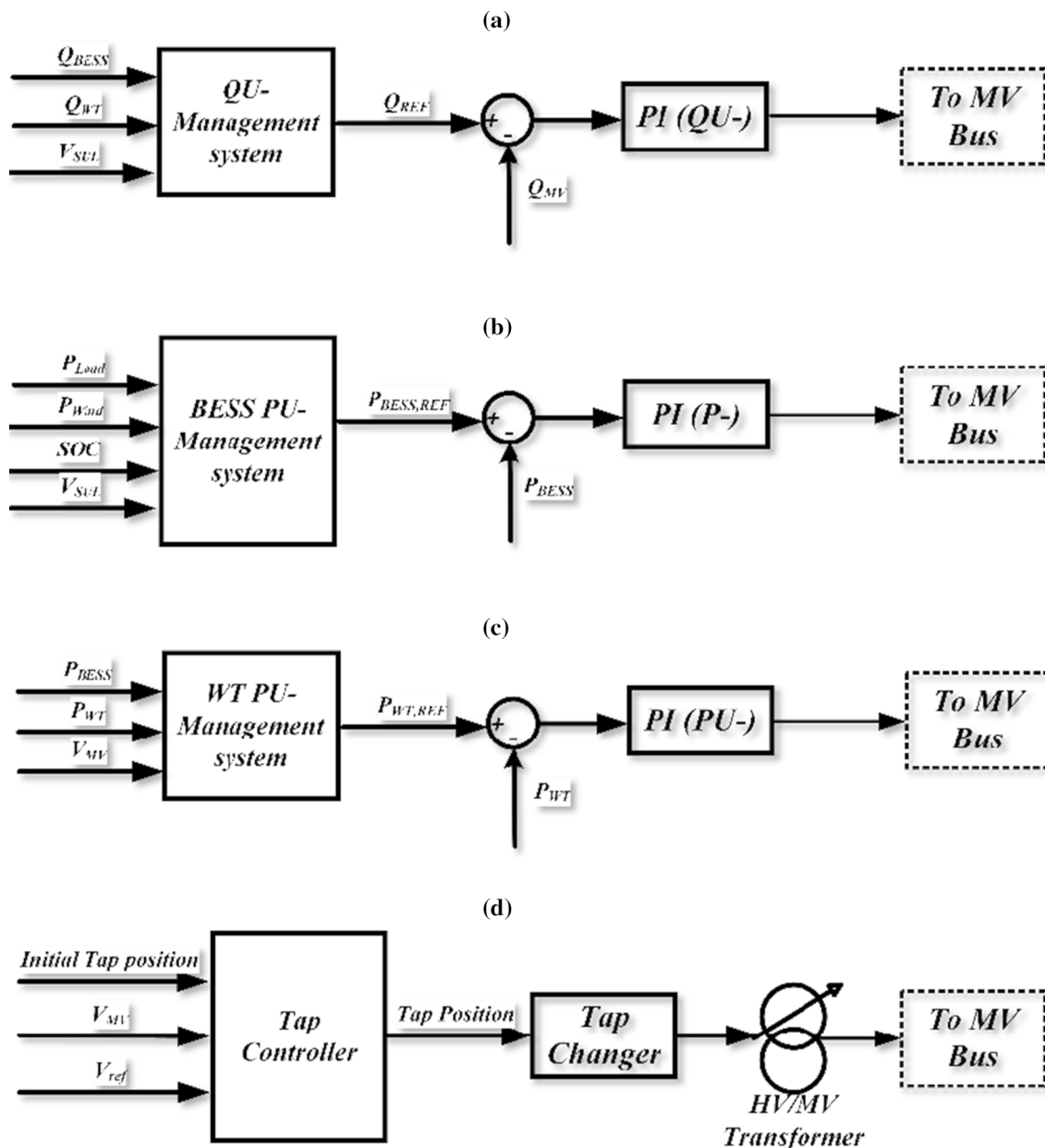
Fig. 6 **a** QU- control, **b** BESS *PU-* control, **c** WT *PU-* control, **d** Tap change controller

Q_{flex}, the flexible reactive power allotted for *QU-* control is based on (19), whose values are in turn dependant on RPW limits defined in Fig. 3. Q_{flex} dispatch is provided by Q_{WIND} and Q_{BESS} whose magnitudes are defined in Eqs. (20) and (21), respectively. The controller is designed in such a way that the Q_{flex} allocated shall control the reactive power flow in the TSO/DSO interface within $Q_{\text{RPW,MIN}}$ and $Q_{\text{RPW,MAX}}$ and the Voltage at Sulva feeder, U_{SUL} which is considered as the reference MV voltage. U_{SUL} has been under stress during the defined use cases, and the Q_{flex} flow addressed to regulate this voltage within grid codes.

4.3.2 BESS *PU-* management system

This paper proposes an autonomous *PU-* droop control scheme for the autonomous operation of the Li-ion BESSs according to voltage measurements at the MV distribution system. The *PU-* control loop is shown in Fig. 7. It is noted that the reactive power control loop has been decoupled from its active power control loop. The error between measured voltage at connection point and the reference voltage value (here it is considered 0.95 pu) is sent to a PI- controller. The droop value is used as negative feedback gain as shown in
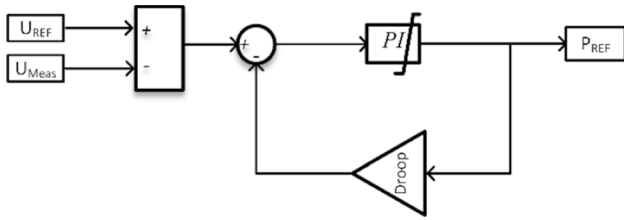
Fig. 7 Droop control loop

Fig. 7. The droop gain of the regulator is set to 0.015 pu (1.5%) per 1 MW. This is a design parameter, which depends on installed network parameters (mention equations) and designed BESS rated power. In this work, the designed system is able to compensate maximum of $\pm 1.5\%$ voltage drifts.

Figure 8 shows this droop characteristic which has been used in this work. In order to avoid oscillation and instability issues, a $\pm 0.5\%$ margin has been considered in order to enable/disable the droop control loop as it is illustrated in Fig. 2. The Li-ion BESSs start to discharge power if the reference voltage from the MV bus goes below 0.95 pu and the discharge power is based on the droop coefficient chosen in the study. In case the WT is non-operational, the Li-ion BESS starts to charge when the voltages rise to 1.05 pu or above. In case the WTG is operational, power generation is curtailed based on its own PU- droop control.

BESS internal control algorithms are described by (22) and (23). Battery discharge power (P_{DIS}) is provided by the BESS system when U_{SUL} is lesser than 0.95 pu, and the magnitude of P_{DIS} is provided by droop characteristics. According to (22), Li-ion BESS will discharge only when its SOC is greater than SOC_{MIN} adhering to the limitations presented by the battery operational characteristics. Maximum P_{DIS} has been set at 1C, i.e. 1 MW. Li-ion BESS charging (P_{CHG}) is defined by the battery's SOC and must be within their threshold SOC_{MIN} and SOC_{MAX} as in (23). Li-ion
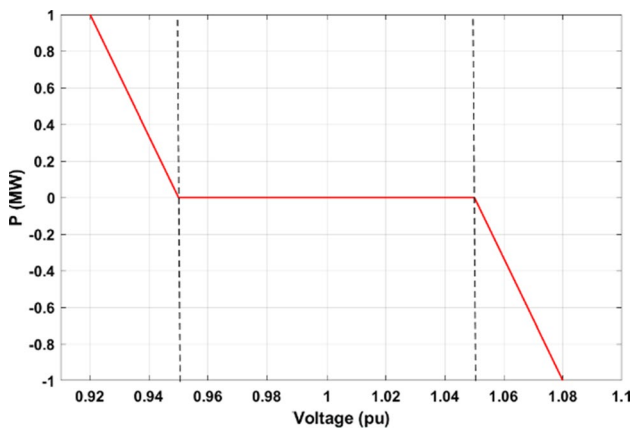
BESS charging is forbidden when BESS SOC is higher than SOC_{MAX}. Magnitude of P_{CHG} is set at a charging rate up to 2C, mainly to observe the MV distribution characteristics when BESS is in different charging modes.

4.3.3 WT *PU-* management system

WT *PU-* management system is designed keeping in mind the curtailment of renewable energy generation, when the voltage limits exceed 1.05 PU in the MV bus of the system. In order to manage the curtailment, droop control referred in Fig. 9 is utilized for the curtailment of wind power generation.

4.3.4 OLTC tap controllers

In the developed ANM scheme, OLTCs are activated to regulate voltages when *QU-*, *QU-* and *P-* controllers fail to provide the required voltage regulation defined by the grid codes in the MV distribution system. OLTC controller receives initial tap position, U_{MV} and U_{REF} V_{ref} as inputs. In order to maintain the MV feeder voltages within the grid codes, U_{REF} V_{ref} of 1 pu is given as input, i.e. U_{MV} V_{MV} V_{MV} is meant to be controlled at 1 pu. Based on V_{ref} U_{REF} and U_{MV} V_{MV} V_{MV} required tap changes are calculated and executed by regulating the voltage at the MV side of the HV/MV transformer.

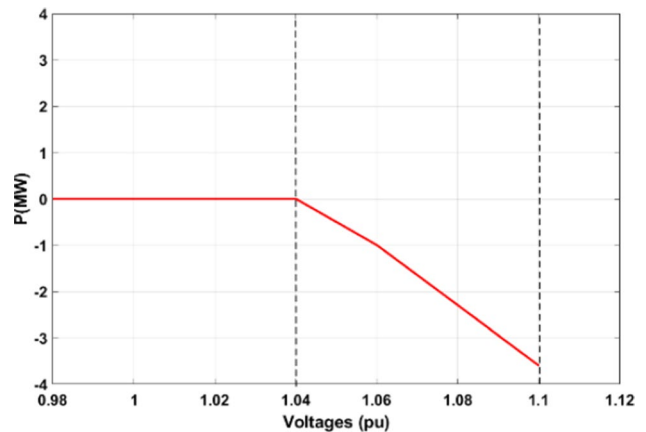
Fig. 8 Li-ion BESS PU- droop characteristics

Fig. 9 WT PU- droop settings

5 Case study: variable load at low WT generation

SSG has been reliable in operation in terms of MV voltage regulation and its power quality during normal mode of operation, i.e. when the grid power is being fed from Sundom HV/MV sub-stations. However, during Sundom HV/MV substation maintenance operation, the grid power will be fed from Kuutamolahti power station (as in Fig. 10) which is about 5.2 KMs away, adding on to the overall Z_{Grid} values. Hence, grid disturbances in the form of voltage fluctuations and power quality problems shall
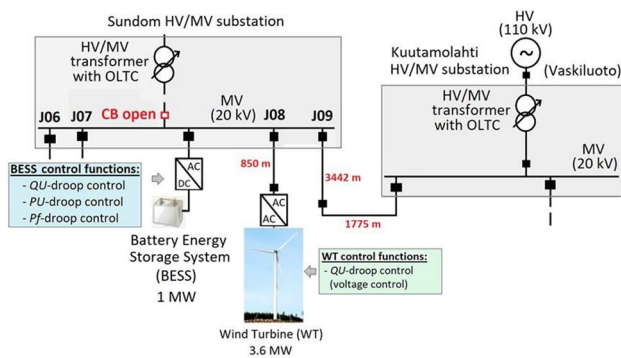

Fig. 10 SSG one-line diagram during backup feeding case

be anticipated, especially when variable load conditions exist at low WTG.

Hence, in this use case, effect of such load variation during lower WT generation during backup feeding case has been modelled. The arising network issues, such as voltage distortion and reactive power flow within RPW, will be addressed by the ANM scheme designed in Sect. 4. The effectiveness of developed ANM scheme and the interaction between EMS and DER controllers during this condition has been studied in detail, considering the Li-ion BESS integration aspects. Initial battery SoC was maintained at about 50%, where it could accommodate simultaneous charge/discharge operations. Characteristics of new cells, i.e. unaged cells are considered for the case study. Simulations were performed for a time period (TS) of 120 s.

5.1 Without ANM

Figure 11a shows the P_{BESS} and Q_{BESS} characteristics of the Li-ion BESS from its MV feeder (J10). Without ANM scheme being active, it is observed that both P_{BESS} and Q_{BESS} are at zero values. P_{WIND} is shown in Fig. 11b and the Q_{WIND} contribution from wind turbine has been unused in the base case evaluation. Figure 11c depicts the active power characteristics at the MV side of the HV/MV transformer. Negative symbol states that the active power is consumed
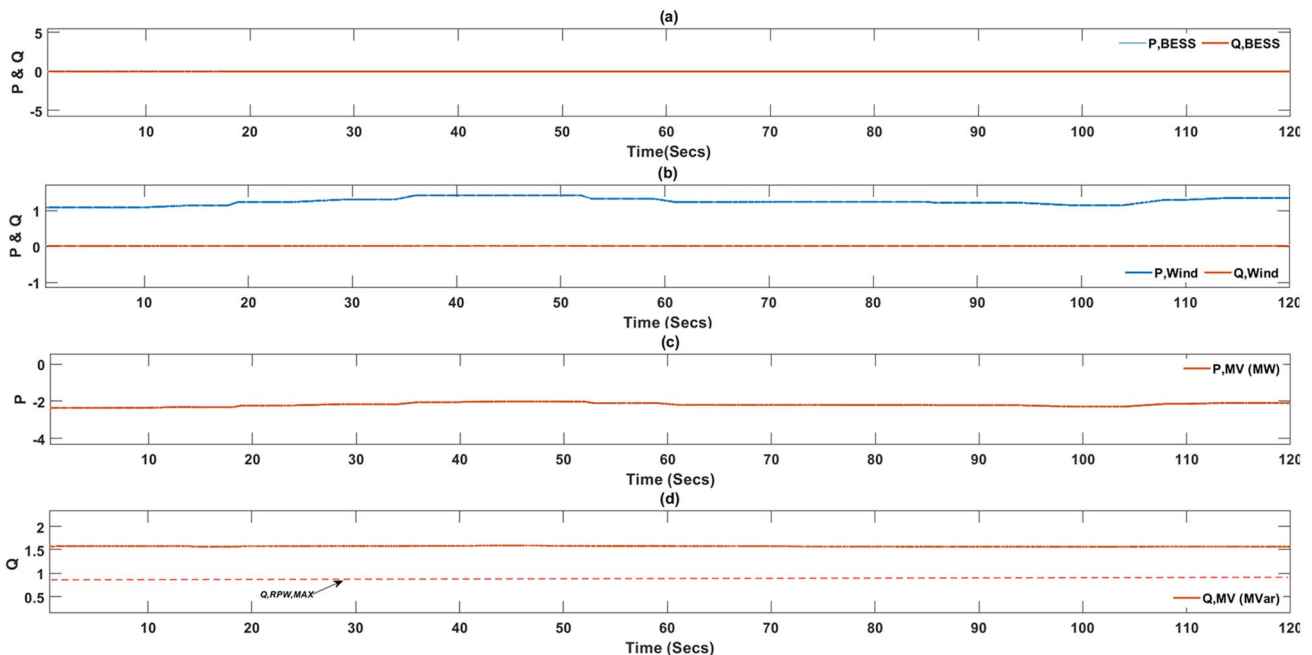

Fig. 11 Case study results (Without ANM): **a** BESS active and reactive power characteristics, **b** Wind active and reactive power characteristics, **c** MV bus active power, **d** MV bus reactive power
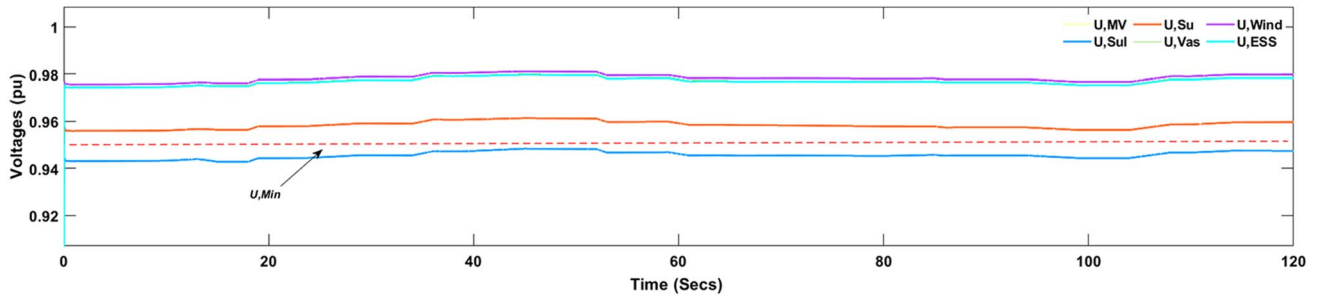
Fig. 12 Case study results (Without ANM): MV bus voltages

by the MV distribution system. Reactive power characteristics are shown in Fig. 11d. It is observed that the Q_{MV} is higher than the threshold defined by the RPW limits set by FINGRID.

Figure 12 represents the voltages in PU at the various MV feeders in the MV distribution system of SSG. It is observed that the voltages are well within the threshold defined by the grid codes, except the voltage at the Sulva feeder. U_{SUL} is seen to be lower than 0.95 PU during the simulation time period.

5.2 With ANM

Figure 13a shows the P_{BESS} and Q_{BESS} characteristics of the Li-ion BESS from its MV feeder (J10) with ANM scheme being active. Magnitude of Li-ion BESS discharge (whose

maximum is set at 1 MW) of P_{BESS} is defined by the BESS *PU*-controller characteristics of the EMS designed to implement ANM scheme, as explained in Sect. 4.3.2. P_{WIND} and Q_{WIND} characteristics are as shown in Fig. 13b. The magnitude of Q_{flex} required to satisfy RPW requirements is shown in (17). The Q_{WIND} contribution as part of Q_{flex} is determined by (18). In this case, Q_{WIND} was alone enough to regulate RPW requirement. Hence, Q_{BESS} dispatch based on (19) was unused. Figure 13c depicts the active power characteristics at the MV side of the HV/MV transformer. Negative symbol states that the active power is consumed by the MV distribution system. Reactive power characteristics are shown in Fig. 13d. It is observed that the Q_{MV} has been reduced in magnitude and currently well within the threshold defined by the RPW limits from Fingrid.
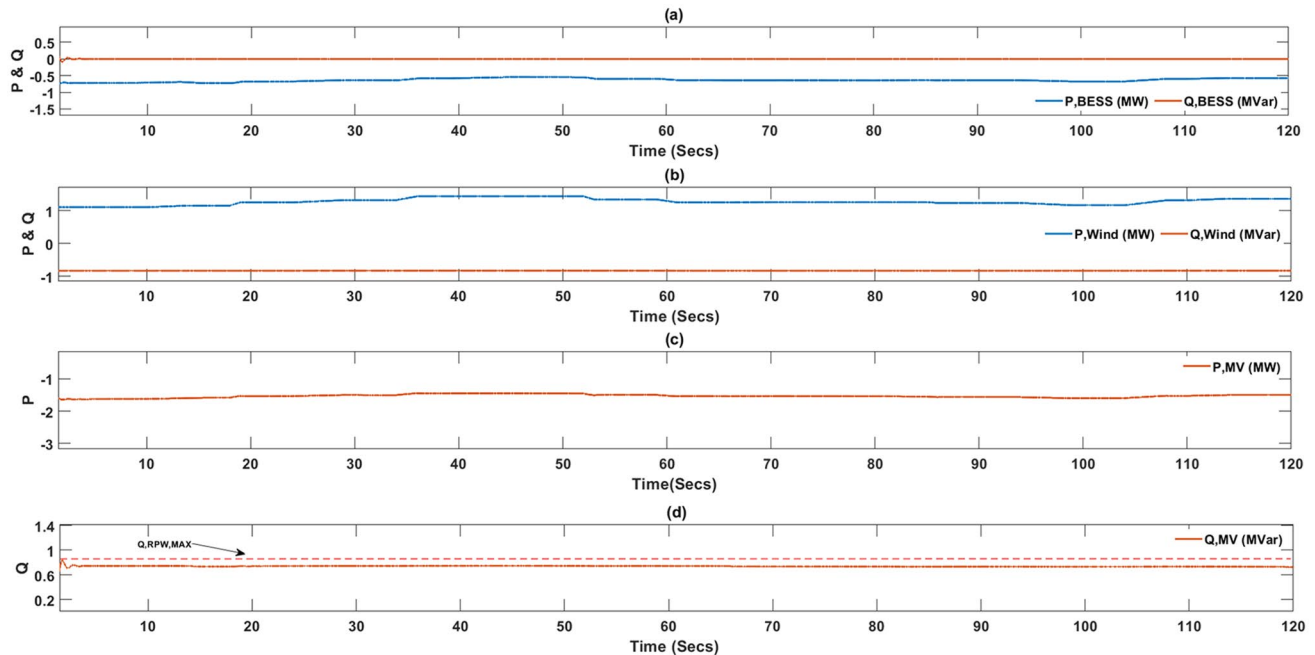

Fig. 13 Case study results (With ANM): **a** BESS active and reactive power characteristics, **b** Wind active and reactive power characteristics, **c** MV bus active power, **d** MV bus reactive power
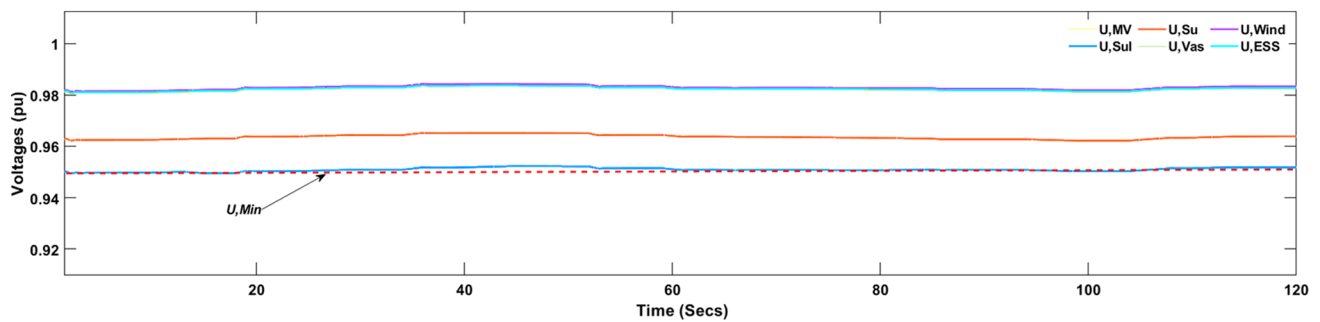
Fig. 14 Case study results (With ANM): MV bus voltages

Fig. 15 BESS DC characteristics: **a** BESS current, **b** BESS voltage, **c** BESS SoC, **d** DC bus voltage
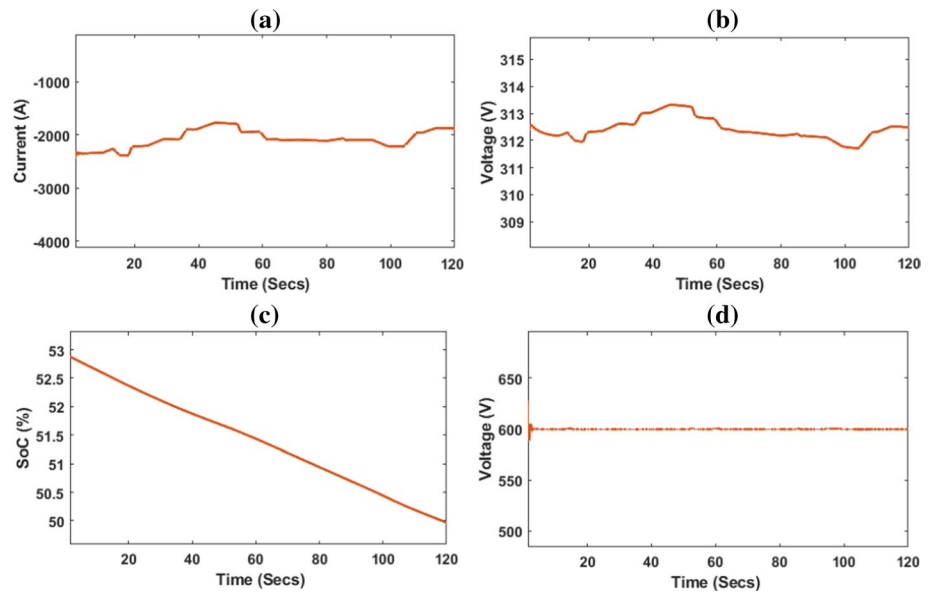

Figure 14 represents the voltages in pu at the various MV feeders in the MV distribution system of SSG. It is observed that the voltages are well within the threshold defined by the grid codes, except the voltage at the Sulva feeder. U_{SUL} was seen to be lower than 0.95 PU in the beginning of the simulation in the base case evaluation. However, all the MV feeder voltages have improved and well within the voltage limits determined by the grid codes after the EMS dispatched required amounts of flexibility (i.e. P_{BESS} and Q_{WIND}).

Figure 14 explains the DC characteristics of the Li-ion BESS and its adjoining PE converters for MV grid codes, except the voltage at the Sulva feeder. U_{SUL} was seen to be lower than 0.95 PU in the beginning of the simulation in the base case evaluation. However, all the MV feeder voltages have improved and well within the voltage limits determined by the grid codes after the EMS dispatched required amounts of flexibility (i.e. P_{BESS} and Q_{WIND}).

Figure 15 explains the DC characteristics of the Li-ion BESS and its adjoining PE converters for MV grid integration. BESS charge/discharge current characteristics are shown in Fig. 15a, where magnitude of defined BESS current, in this case, is the BESS discharge current. Figure 15b depicts the changes in BESS operational voltage. BESS SoC behaviour is presented in Fig. 15c. DC-bus voltage is constantly maintained at 600 V, despite frequent variation in BESS voltage and Fig. 15d, thereby, reinforcing robust BESS model and adjoining converter controller integration design for 1 MW charge power.

6 Discussion and conclusion

Role of Li-ion BESSs as flexible energy sources in such distribution networks is multi-faceted considering their participation in both active and reactive power related flexibility services. In this study, the developed Li-ion BESS

integration was subjected to the load requirements of ANM schemes in the MV distribution system of SSG, when the WT generation was low and variable load conditions exist. Under such situation, transient instability is seen in the network in terms of voltage regulation. Also, the RPW limits defined by the grid codes are non-adhering to the threshold values. It is imperative that the developed EMS and its adjoining controllers must work in a co-ordinated way with the DER inverter controllers, i.e. Li-ion BESS and the WT generator in order to satisfy the ANM objectives.

Li-ion BESS integration design was validated as a part of the use case. DC/AC voltage source converter and DC/DC bidirectional buck-boost converter and their respective controllers used in the Li-ion BESS performed as per the load requirements provided by the ANM scheme to contain voltage and RPW violation. The stability of the DC bus in Fig. 15d aids in validating the Li-ion BESS integration design being stable even at various transient conditions despite variable WTG and loads.

Table 1 provides a summary of the simulation results and an indication on how the flexibility indices have been utilized based on the ANM objectives and the EMS set-points based on Eqs. (17)–(23). The reactive power control requirement, Q_{flex}, has been provided only by Q_{WIND}, without any interference from Q_{BESS}. From the results, it is indicative that the Q_{flex}, based on (17), was instrumental in keeping the reactive power flow, Q_{MV} between HV/MV grids, within the limits specified by the RPW. With respect to the results of voltage limits at various MV feeders, it has been evident that the voltage at the Sulva feeder was below 0.95 pu without any ANM schemes operational. However, with the allocation of P_{BESS}, whose dispatch value was based on the BESS *PU*-droop controller characteristics, voltage at the Sulva feeder was controlled at 0.95 pu. Purpose of this control loop is to dispatch the exact amount of active power required from the Li-ion BESS which is derived in Sect. 3, where the Li-ion BESS dispatch is dictated by (15), thereby providing optimum power without over/under- usage of the battery system.

The synergy between Li-ion BESS converter controls and the EMS controllers (i-e. BESS *PU-* and *QU-* controllers) has been established as a part ANM design and validated by the simulation results, where the EMS controllers provided required set-points to the individual component (Li-ion BESS and WTG) controllers. Therefore, the designed ANM scheme and its adjoining EMS controllers acted as required to provide RPW and voltage regulation.

In future studies, more use cases such as such as complementing RES intermittency and frequency fluctuations, will be added to the existing ANM control architecture, particularly focusing on the multi-use capability of the Li-ion BESSs. Design and development of adaptive EMS controllers to optimise the control of flexible energy sources in MV distribution systems will be included in the scope of study.

Table 1 Results summary (mapping flexibility indices)

Simulation step	5 s		20 s		40 s		60 s		80 s		100 s		120 s	
Flexibility indices	No ANM	ANM	No ANM	ANM	No ANM	ANM	No ANM	ANM	No ANM	ANM	No ANM	ANM	No ANM	ANM
P_{BESS} (MW)	0	-0.71	0	-0.67	0	-0.57	0	-0.61	0	-0.64	0	-0.67	0	-0.57
Q_{BESS} (Mvar)	0	0	0	0	0	0	0	0	0	0	0	0	0	0
Q_{WIND} (Mvar)	0	-0.83	0	-0.83	0	-0.83	0	-0.83	0	-0.83	0	-0.83	0	-0.83
Q_{flex} (Mvar)	0	-0.83	0	-0.83	0	-0.83	0	-0.83	0	-0.83	0	-0.83	0	-0.83
Q_{MV} (pu)	1.56	0.73	1.56	0.73	1.56	0.73	1.56	0.73	1.56	0.73	1.56	0.73	1.56	0.73
U_{SUL} (pu)	0.943	0.95	0.944	0.95	0.947	0.951	0.946	0.951	0.945	0.95	0.944	0.95	0.947	0.951

Further, real-time simulation models shall be built for EMS controller test-bed development purposes.

References

1. Pinson P, Mitridati L, Ordoudis C, Ostergaard J (2017) Towards fully renewable energy systems: Experience and trends in Denmark. CSEE J Power Energy Syst 3:26–35. https://doi.org/10.17775/cseejpes.2017.0005

2. Liang X (2017) Emerging power quality challenges due to integration of renewable energy sources. IEEE Trans Ind Appl 53:855–866. https://doi.org/10.1109/TIA.2016.2626253

3. Ahmed SD, Al-Ismail FSM, Shafiullah M et al (2020) Grid integration challenges of wind energy: a review. IEEE Access 8:10857–10878. https://doi.org/10.1109/ACCESS.2020.2964896

4. Gao X, Sossan F, Christakou K et al (2018) Concurrent voltage control and dispatch of active distribution networks by means of smart transformer and storage. IEEE Trans Ind Electron 65:6657–6666. https://doi.org/10.1109/TIE.2017.2772181

5. Yang Z, Li Y, Xiang J (2018) Coordination control strategy for power management of active distribution networks. IEEE Trans Smart Grid 10:5524–5535. https://doi.org/10.1109/TSG.2018.2883987

6. Palizban O, Kauhaniemi K, Guerrero JM (2014) Microgrids in active network management—part II: system operation, power quality and protection. Renew Sustain Energy Rev 36:440–451. https://doi.org/10.1016/j.rser.2014.04.048

7. Palizban O, Kauhaniemi K, Guerrero JM (2014) Microgrids in active network management—Part I: hierarchical control, energy storage, virtual power plants, and market participation. Renew Sustain Energy Rev 36:428–439. https://doi.org/10.1016/j.rser.2014.01.016

8. Salama HS, Aly MM, Abdel-Akher M, Vokony I (2019) Frequency and voltage control of microgrid with high WECS penetration during wind gusts using superconducting magnetic energy storage. Electr Eng 101:771–786. https://doi.org/10.1007/s00202-019-00821-w

9. Böhm R, Rehtanz C, Franke J (2016) Inverter-based hybrid compensation systems contributing to grid stabilization in medium voltage distribution networks with decentralized, renewable generation. Electr Eng 98:355–362. https://doi.org/10.1007/s00202-016-0425-y

10. Olek B, Wierzbowski M (2015) Local energy balancing and ancillary services in low-voltage networks with distributed generation, energy storage, and active loads. IEEE Trans Ind Electron 62:2499–2508. https://doi.org/10.1109/TIE.2014.2377134

11. Wang L, Bai F, Yan R, Saha TK (2018) Real-time coordinated voltage control of PV inverters and energy storage for weak networks with high PV penetration. IEEE Trans Power Syst 33:3383–3395. https://doi.org/10.1109/TPWRS.2018.2789897

12. Akagi S, Yoshizawa S, Ito M et al (2020) Multipurpose control and planning method for battery energy storage systems in distribution network with photovoltaic plant. Int J Electr Power Energy Syst 116:105485. https://doi.org/10.1016/j.ijepes.2019.105485

13. Das CK, Bass O, Kothapalli G et al (2018) Overview of energy storage systems in distribution networks: placement, sizing, operation, and power quality. Renew Sustain Energy Rev 91:1205–1230. https://doi.org/10.1016/j.rser.2018.03.068

14. Saboori H, Hemmati R, Ghiasi SMS, Dehghan S (2017) Energy storage planning in electric power distribution networks—a state-of-the-art review. Renew Sustain Energy Rev 79:1108–1121. https://doi.org/10.1016/j.rser.2017.05.171

15. Zhang Y, Xu Y, Yang H, Dong ZY (2019) Voltage regulation-oriented co-planning of distributed generation and battery storage in active distribution networks. Int J Electr Power Energy Syst 105:79–88. https://doi.org/10.1016/j.ijepes.2018.07.036

16. Akram U, Nadarajah M, Shah R, Milano F (2020) A review on rapid responsive energy storage technologies for frequency regulation in modern power systems. Renew Sustain Energy Rev 120:109626. https://doi.org/10.1016/j.rser.2019.109626

17. Nour AMM, Hatata AY, Helal AA, El-Saadawi MM (2020) Review on voltage-violation mitigation techniques of distribution networks with distributed rooftop PV systems. IET Gener Transm Distrib 14:349–361. https://doi.org/10.1049/iet-gtd.2019.0851

18. Liu J, Gao H, Ma Z, Li Y (2015) Review and prospect of active distribution system planning. J Mod Power Syst Clean Energy 3:457–467. https://doi.org/10.1007/s40565-015-0170-7

19. Sirvio K, Valkkila L, Laaksonen H et al (2018) Prospects and costs for reactive power control in Sundom smart grid. In: Proceedings of 2018 IEEE PES Innov Smart Grid Technol Conf Eur ISGT-Europe 2018, pp 1–6. https://doi.org/10.1109/ISGTEurope.2018.8571695

20. Sirviö K, Laaksonen H, Kauhaniemi K (2020) Active network management scheme for reactive power control. In: 7–8 Cired Workshop 2018. https://www.cired-repository.org/handle/20.500.12455/1099

21. Laaksonen H, Hovila P, Kauhaniemi K (2018) Combined islanding detection scheme utilising active network management for future resilient distribution networks. J Eng 2018:1054–1060. https://doi.org/10.1049/joe.2018.0202

22. Laaksonen H, Sirviö K, Aflecht S, Kauhaniemi K (2019) Multi-objective active network management scheme studied in Sundom smart grid with MV and LV connected DER Units. 3–6, Cired 2019 conference. https://doi.org/10.34890/379

23. Laaksonen H, Parthasarathy C, Hafezi H et al (2020) Control and management of distribution networks with flexible energy resources. Int Rev Electr Eng 15:213. https://doi.org/10.15866/iree.v15i3.18592

24. European Union (2016) DCC: Commission Regulation (EU) 2016/1388 establishing a network code on Demand Connection. Off J Eur Union 2016:68. doi:https://doi.org/10.1017/CBO9781107415324.004

25. Li C, Disfani VR, Pecenak ZK et al (2018) Optimal OLTC voltage control scheme to enable high solar penetrations. Electr Power Syst Res 160:318–326. https://doi.org/10.1016/j.epsr.2018.02.016

26. Muttaqi KM, Le ADT, Negnevitsky M, Ledwich G (2015) A coordinated voltage control approach for coordination of OLTC, voltage regulator, and DG to regulate voltage in a distribution feeder. IEEE Trans Ind Appl 51:1239–1248. https://doi.org/10.1109/TIA.2014.2354738

27. Long C, Ochoa LF (2016) Voltage control of PV-rich LV networks: OLTC-fitted transformer and capacitor banks. IEEE Trans Power Syst 31:4016–4025. https://doi.org/10.1109/TPWRS.2015.2494627

28. Zia MF, Elbouchikhi E, Benbouzid M (2018) Microgrids energy management systems: a critical review on methods, solutions, and prospects. Appl Energy 222:1033–1055. https://doi.org/10.1016/j.apenergy.2018.04.103

29. Parthasarathy C, Hafezi H, Laaksonen H, Kauhaniemi K (2019) Modelling and simulation of hybrid PV & BES systems as flexible resources in smartgrids—Sundom smart grid case. In: IEEE PES PowerTech Conf 2019. https://doi.org/10.1109/PTC.2019.8810579

30. Parthasarathy C, Hafezi H, Laaksonen H (2020) Lithium-ion BESS Integration for Smart Grid Applications—ECM modelling approach ISGT NA. https://doi.org/10.1109/ISGT45199.2020.9087741

31. Li B, Chen M, Cheng T et al (2018) Distributed control of energy-storage systems for voltage regulation in distribution network with high PV penetration. In: 2018 UKACC 12th Int Conf Control Control 2018 9:169–173. https://doi.org/10.1109/CONTROL.2018.8516803

32. COMMISSION REGULATION (EU) 2016/ 631 - of 14 April 2016 - establishing a network code on requirements for grid connection of generators http://data.europa.eu/eli/reg/2016/631/oj

Publisher's Note Springer Nature remains neutral with regard to jurisdictional claims in published maps and institutional affiliations.